

1 Surrogate-based pumping optimization of coastal aquifers under limited computational 2 budgets

3 Vasileios Christelis^{1,*}, Rommel G. Regis², Aristotelis Mantoglou¹

4 ¹ Laboratory of Reclamation Works and Water Resources Management, School of Rural and
5 Surveying Engineering, National Technical University of Athens, Athens, Greece

6 ² Department of Mathematics, Saint Joseph's University Philadelphia, USA

7 Corresponding author: Vasileios Christelis (vchrist@survey.ntua.gr)

8 * British Geological Survey, Environmental Science Centre, Keyworth, Nottingham, UK

9 Abstract

10 The long runtimes of variable density and salt transport numerical models hinder the
11 implementation of simulation-optimization routines for coastal aquifer management. To reduce
12 this excessive computational cost, surrogate models have been successfully applied in several
13 studies. However, it has not been previously addressed how effective is surrogate modelling in
14 pumping optimization of coastal aquifers, given a limited number of available runs with the
15 seawater intrusion model. To that end, two surrogate-based optimization frameworks are
16 employed and compared against the direct optimization approach under restricted
17 computational budgets. The first surrogate-assisted algorithm, utilizes an infill strategy aiming
18 at a fast local improvement of the surrogate model around optimal values. The other, balances
19 global and local improvement of the surrogate model while it is applied for the first time in
20 coastal aquifer management. The performance of the algorithms is investigated for
21 optimization problems of moderate and large dimensionality. Results indicate that for all
22 problems, the surrogate-based optimization methods provide higher objective function values
23 than the direct optimization. Additionally, the selection of cubic radial basis function surrogate
24 models, enables the construction of very fast approximations for problems with up to 40
25 decision variables and 40 constraint functions.

26

27

28

29

30

31

32

33

34 **INTRODUCTION**

35

36 Variable density and salt transport (VDST) numerical models are indispensable tools for
37 simulating seawater intrusion (SWI) in coastal aquifers (Werner *et al.* 2013). They have been
38 effectively employed to improve understanding in real-world SWI problems (e.g. Gingerich &
39 Voss 2005; Giambastiani *et al.* 2007; Kopsiaftis *et al.* 2009; Kerrou *et al.* 2013). Additionally,
40 the simulation of dispersive flow between seawater and freshwater by using VDST models,
41 enables a more accurate management of groundwater abstraction in coastal aquifers (Pool and
42 Carrera , 2011).

43 However, VDST models are computationally expensive, as is the case with most of the high-
44 fidelity computer simulations. Hence, their use in iterative numerical tasks, such as sensitivity
45 analysis or optimization, is hindered by the increased computational cost. To address this issue,
46 several studies have employed data-driven surrogate modelling techniques either to partly or
47 fully replace the computationally expensive VDST simulations (Sreekanth & Datta 2015).
48 Examples of surrogate models in coastal aquifer management comprise artificial neural
49 networks (e.g. Rao *et al.* 2004; Bhattacharjya & Datta 2005; Kourakos & Mantoglou 2009;
50 Ataie-Ashtiani *et al.* 2013; Kourakos & Mantoglou 2013; Roy *et al.* 2016), genetic
51 programming (Sreekanth & Datta 2011), evolutionary polynomial regression (Hussain *et al.*
52 2015), polynomial chaos expansions (Rajabi *et al.* 2015), radial basis functions (Christelis &
53 Mantoglou 2016a) or fuzzy inference systems (Roy & Datta 2016).

54 Typically, an initial set of input-output data from the physics-based models is used to train
55 the surrogate models in order to attain a certain level of accuracy for predicting responses to
56 unseen data (Solomatine & Ostfeld 2008). It is unlikely though that a global accurate surrogate
57 model can be constructed, given that the number of available runs with the original model is
58 usually limited due to computational restrictions (Forrester *et al.* 2008). In certain coastal
59 aquifer management studies, hundreds to thousands input-output patterns were used to
60 construct an accurate surrogate model (Sreekanth & Datta 2015). The use of large training
61 patterns may lead to impractical computational cost even for a VDST model with simulation
62 runtimes of few minutes.

63 Most coastal aquifer management studies, have applied surrogate-based optimization (SBO)
64 methods without pre-specified restrictions on the overall computational budget. The use of
65 adaptive surrogate training frameworks has significantly reduced the associated computational
66 burden (e.g. Kourakos & Mantoglou 2009; Papadopoulou *et al.* 2010; Christelis & Mantoglou
67 2016a). Alternatively, Ataie-Ashtiani *et al.* (2014) proposed a zonation methodology as a
68 practical approach to reduce the dimensionality of the optimization problem and therefore the

69 required training data for building the surrogate models. It is also worth noting that pumping
70 optimization problems of coastal aquifers usually involve non-linear constraints (Mantoglou *et*
71 *al.* 2004). The presence of non-linear constraints further complicates the development of SBO
72 methods (Forrester *et al.* 2008).

73 Nevertheless, many engineering optimization studies have focused on approximating the
74 global optimum based on a specified number of runs with the original expensive computer
75 model. There is a wide body of SBO literature which develops adaptive sampling strategies
76 that effectively utilize the expensive original model runs, to update the surrogate and increase
77 its accuracy within regions of interest (e.g. Jones 1998; Mugunthan *et al.* 2005; Regis &
78 Shoemaker 2007; Forrester & Keane 2009; Parr *et al.* 2012; Regis & Shoemaker 2013; Regis
79 2014; Tsoukalas *et al.* 2016). However, the application of comprehensive SBO strategies which
80 exploit information from the surrogate models in order to sample the expensive original model
81 is rather limited in groundwater modelling and optimization (Asher *et al.* 2015). Furthermore,
82 it is debatable if there is a benefit from the use of surrogate models in optimization problems
83 with increased dimensionality and under limited computational budgets (Razavi *et al.* 2012a).

84 In the present paper, we address the effectiveness of surrogate modelling in pumping
85 optimization of coastal aquifers, given a limited number of available runs with the expensive
86 SWI model. Two SBO frameworks are employed in order to solve single-objective pumping
87 optimization problems. The first SBO algorithm utilizes a metamodel-embedded evolution
88 framework which constructs radial basis function (RBF) surrogate models for the constraints
89 functions only. RBF surrogate models have been successfully applied in several SBO
90 optimization problems (Razavi *et al.* 2012b). The other is an advanced SBO algorithm, namely,
91 ConstrLMSRBF (Regis, 2011), which simultaneously deals with the objective function and the
92 constraints of the optimization problem, by constructing RBF surrogate models for each one
93 of them. ConstrLMSRBF algorithm is applied for the first time in water resources optimization
94 and for problems of pumping optimization of coastal aquifers. The goal of this study is to
95 investigate the performance of these SBO algorithms on different dimensionalities of the
96 decision variable space while imposing strong restrictions on the number of available runs with
97 the VDST model. The latter assumption is closer to real-world cases where coastal aquifer
98 management problems involve computationally heavy numerical models of SWI. The SBO
99 algorithms are compared against direct optimization with the VDST model in order to evaluate
100 the usefulness of constructing surrogate models in the case of limited computational budgets.

101 The rest of the paper includes 4 sections. Section 2 presents the SWI numerical simulation
102 model, the coastal aquifer model and the formulation of the pumping optimization problem. In

103 section 3 the surrogate models along with their implementation in SBO strategies are described.
 104 Section 4 presents the optimization results and finally section 5 concludes on the findings of
 105 the present study.

106

107 **METHODS**

108

109 **SWI modelling**

110

111 VDST models utilize numerical codes which solve a coupled system of partial differential
 112 equations of flow and transport in order to simulate SWI (Voss & Souza 1987). It is considered
 113 a complicated and computationally expensive numerical task mostly due to the spatial and time
 114 discretization requirements of the solute transport step (Werner *et al.* 2013). In the present
 115 paper, the HydroGeoSphere code (HGS) (Therrien & Sudicky 1996; Graf & Therrien 2005;
 116 Therrien *et al.* 2006) was used to simulate SWI. The HGS code applies the control volume
 117 finite element method with adaptive time-stepping while a Picard iteration scheme is utilized
 118 to iteratively solve the system of flow and transport equations for VDST simulations
 119 (Thompson *et al.* 2007). The mathematical formulation of VDST modelling is briefly described
 120 below whereas comprehensive presentations can be found elsewhere (e.g. Kolditz *et al.* 1998).

121

$$122 \quad \frac{\partial}{\partial x_i} \left[K_{ij} \left(\frac{\partial h_f}{\partial x_j} + \rho_r n_j \right) \right] + Q_\rho = S_s \frac{\partial h_f}{\partial t} \quad (1)$$

123

124

$$125 \quad \frac{\partial}{\partial x_i} \left(D_{ij} \frac{\partial c}{\partial x_j} - q_i c \right) + Q_c = \frac{\partial(\phi c)}{\partial t} \quad (2)$$

126

127 In the flow equation (1) the equivalent freshwater head h_f [L] is the flow variable given by
 128 $h_f = (p/\rho_f g) + z$, where p [$ML^{-1}T^{-2}$] is the fluid pressure, ρ_f [ML^{-3}] is the reference fluid
 129 density, g [ML^{-2}] is the gravity acceleration constant and z [L] is the elevation above
 130 horizontal datum. The indices i, j represent the unit vectors in x and y directions respectively,
 131 while n_j represents the direction of flow and it equals 1 in the vertical direction and 0 for the

132 horizontal directions. In transport equation (2) the dimensionless relative concentration $c [-]$
 133 is the transport variable which varies between 0 and 1. It is linearly related to fluid density ρ
 134 $[ML^{-3}]$ through $(\rho - \rho_f)/\rho_f = [(\rho_{\max} - \rho_f)/\rho_f]c$, under the assumption that the solute
 135 concentration of a fluid is $c_{\max} = 1$ when $\rho = \rho_{\max}$. The term $(\rho - \rho_f)/\rho_f$ represents the
 136 dimensionless relative density ρ_r . $K_{ij} [LT^{-1}]$ are the coefficients of freshwater hydraulic
 137 conductivity tensor, $D_{ij} [L^2T^{-1}]$ are the coefficients of the dispersion tensor, $\phi [-]$ is porosity,
 138 $t [T]$ is time, $Q_p [L^3L^{-3}T^{-1}]$ is a volumetric fluid source/sink term per unit aquifer volume, Q_c
 139 $[ML^{-3}T^{-1}]$ is a solute mass source/sink term and $S_s [L^{-1}]$ is the specific storage. The Darcy
 140 flux term q_i is expressed for freshwater properties as:

141

$$142 \quad q_i = -K_{ij} \left(\frac{\partial h_f}{\partial x_j} + \rho_r n_j \right) \quad (3)$$

143

144 Coastal aquifer application model

145

146 The numerical SWI simulations are based on a coastal aquifer model of rectangular shape
 147 (figure 1) which is an approximation of a real aquifer at the Greek Island of Kalymnos
 148 (Mantoglou *et al.* 2004).

149

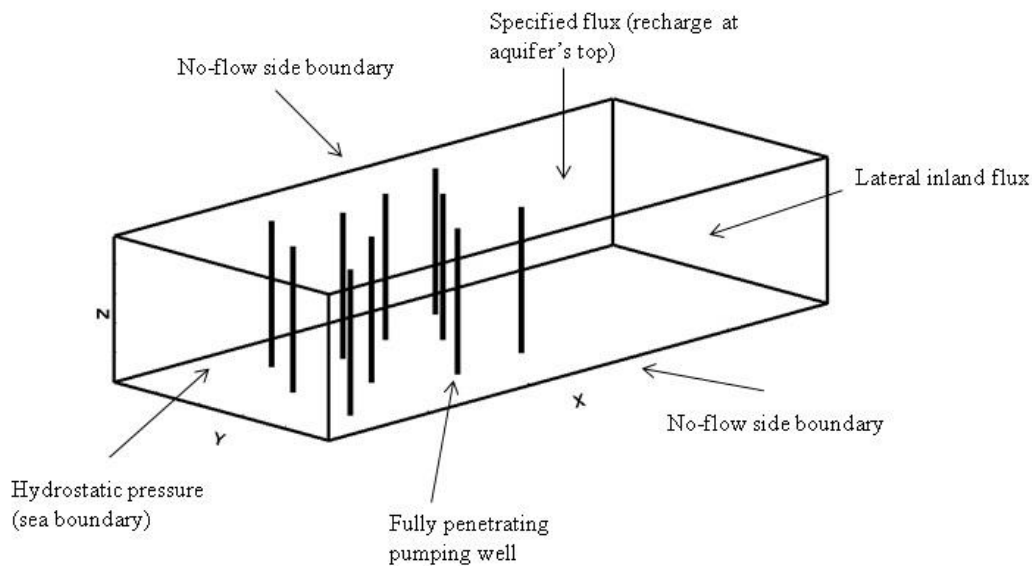
150

151

152

153

154



155

156 [FIGURE 1]

157

158 The horizontal dimensions of the coastal aquifer model are $x = 7000m$, $y = 3000m$ and the
 159 aquifer base is at $z = -25m$ below sea-level. On the west side of the aquifer model a hydrostatic
 160 specified head boundary condition is applied along with a specified salinity concentration of
 161 $35 Kg/m^3$ for a saltwater density of approximately $1025 Kg/m^3$. The aquifer is replenished by
 162 both recharge and inland fluxes. The two lateral boundaries are no-flow boundaries while fully
 163 penetrating pumping wells extract groundwater from the coastal aquifer. A homogeneous and
 164 anisotropic coastal aquifer is assumed where the values of hydraulic conductivity are
 165 $K_x = K_y = 100m/day$ and $K_z = 10m/day$. The longitudinal dispersivity value was set to $100m$
 166 and the transverse dispersivity value to $10m$. In the absence of field data and due to the
 167 exploratory features of this study, relatively large dispersivity values were selected to facilitate
 168 the setup of a faster VDST model since spatial discretization is related to dispersivity values
 169 (Werner *et al.* 2013). Note that for all the optimization problems described in the following
 170 sections, multiple independent optimization runs are performed in order to produce a statistical
 171 output due to the stochastic nature of the algorithms. In that sense, a relatively fast VDST model
 172 is required to realize such a demanding computational task for generic comparison purposes.
 173 A single run of the VDST model required an approximate CPU time of 30 seconds, running on
 174 a 2.53 GHz Intel i5 processor with 6 GB of RAM in a 64-bit Windows 7 system.

175

176

177 Formulation of the pumping optimization problem

178

179 The pumping optimization problem of the present work lies in the category of non-linear
180 constrained optimization problems described as follows:

181

$$\begin{aligned} 182 \quad & \min f(\xi) \\ & \text{s.t. } g_i(\xi) \leq 0, i = 1, 2, \dots, M, l \leq \xi \leq u \end{aligned} \quad (4)$$

183

184 where f, g_i represent the objective function and inequality constraint functions respectively.

185 The vector ξ takes values in the N -dimensional continuous space $[l, u] \subset R^N$. A real vector

186 ξ^* is sought so that $f(\xi^*) = \min f(\xi)$, subject to the constraints defined in equation (4). It is

187 assumed that the derivatives of f, g are not available while the bound constraints define the

188 search space of the optimization problem. The corresponding single-objective pumping

189 optimization problem can be mathematically described as (Mantoglou 2003; Mantoglou *et al.*

190 2004):

191

$$\begin{aligned} & \min - \sum_{i=1}^M Q_i \\ 192 \quad & \text{s.t. } x_i^{c_{\max}}(Q_1, Q_2, \dots, Q_M) \leq xw_i, \forall i = 1, 2, \dots, M \\ & Q_{\min} \leq Q_i \leq Q_{\max}, i = 1, 2, \dots, M \end{aligned} \quad (5)$$

193

194 where Q_i is the individual pumping rate of each pumping well and $x_i^{c_{\max}}$ is the horizontal

195 distance of the iso-salinity c_{\max} from the coast, as a function of pumping rates from each

196 pumping well. The variable xw_i refers to the pumping well location, while Q_{\min} and Q_{\max}

197 define the lower and upper limits which pumping rates can take. The goal is to maximize (the

198 reason for the negative sign in the objective function) the total groundwater extraction, subject

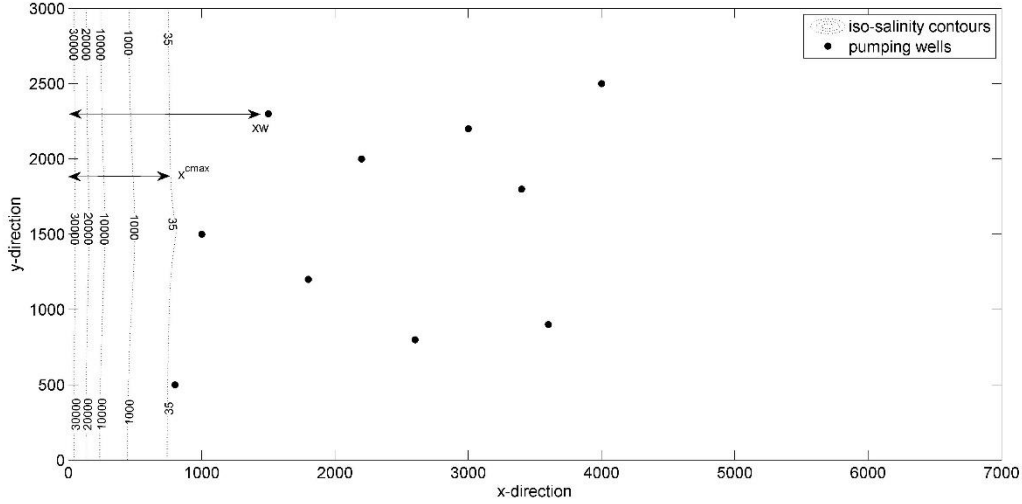
199 to constraints which maintain the salinity levels in pumped groundwater at the specified limit

200 of $c_{\max} = 35 \text{ mg/l}$. Figure 2 illustrates a plan view of the simulated iso-salinity contours at the

201 aquifer base, for a feasible vector Q of pumping rates.

202

203



204

205 [FIGURE 2]

206

207 The optimization problem in (5) can be translated to a bound-constrained optimization
 208 problem using penalty terms in the objective function. Thus, the objective function value is
 209 penalized every time that a constraint of the problem is violated. In this study we have applied
 210 the following objective function penalty formulation:

211

$$212 \min f(Q) = \begin{cases} -\sum_{i=1}^M Q_i, & \text{if } \forall i = 1, 2, \dots, M; x_i^{c\max}(Q_1, Q_2, \dots, Q_M) \leq xw_i \\ M_v \sum_{i=1}^M \left[\max((x_i^{c\max} - xw_i), 0) \right]^2, & \text{if } \exists i = 1, 2, \dots, M; x_i^{c\max}(Q_1, Q_2, \dots, Q_M) > xw_i \end{cases} \quad (6)$$

213

214 where M_v represents the number of pumping wells that the constraint is violated. The above
 215 formulation aims to attribute a separate score for each violated constraint while it involves the
 216 magnitude of violation through the squared difference between $x_i^{c\max}$ and xw_i . The penalized
 217 objective function is also multiplied by M_v to incorporate the number of constraint violations
 218 for a non-feasible vector Q . The pumping optimization problem defined above can be directly
 219 solved using the VDST model combined with a proper optimization algorithm. In pumping
 220 optimization of coastal aquifers, evolutionary algorithms tend to perform better than
 221 conventional gradient-based algorithms which might get trapped in local minima (Ketabchi &
 222 Ataie-Ashtiani 2015). However, evolutionary algorithms require a large number of function
 223 evaluations to converge and their performance may vary depending on the application

224 (Mantoglou & Papantoniou 2008; Karpouzos & Katsifarakis 2013; Ketabchi & Ataie-Ashtiani,
 225 2015). Therefore, the direct solution of pumping optimization problems using VDST models
 226 and evolutionary algorithms may result in excessive computational burden.

227 In this study, a heuristic optimization method, namely, the evolutionary annealing-simplex
 228 (EAS) algorithm (Efstratiadis & Koutsoyiannis, 2002), is utilized to solve the penalized
 229 formulation of the optimization problem defined in (6). EAS algorithm employs the concepts
 230 of evolutionary search, the downhill simplex scheme and simulated annealing (Rozos *et al.*
 231 2004). It has shown a robust performance for various pumping optimization problems of
 232 coastal aquifers (Kourakos & Mantoglou, 2009, Christelis & Mantoglou 2016a, Christelis &
 233 Mantoglou 2016b). Thereinafter, the direct optimization approach with the SWI model will be
 234 referred as VDST-EAS.

235

236 **The surrogate model**

237

238 The VDST-EAS approach may considerably increase the required computational effort to get
 239 an optimal solution. In some cases, the VDST simulations can be very expensive so that only
 240 a small number of them can be utilized to estimate a feasible solution in reasonable
 241 computational times (e.g. Christelis & Mantoglou 2016b). In this section, surrogate models are
 242 proposed as an alternative method for attaining an improved optimal solution based on a
 243 specified number of runs with the VDST model.

244 In the pumping optimization problem described in (5), the objective function is just a linear
 245 function of the decision variables Q_1, Q_2, \dots, Q_M which are the pumping rates, while the
 246 constraint functions are computationally expensive to evaluate. There are a variety of surrogate
 247 modelling techniques that can be used to approximate the constraints, including Kriging, RBF
 248 and Support Vector Machines (SVM). This paper employs a cubic RBF model augmented with
 249 a linear polynomial tail, in order to build a surrogate model for each of the M inequality
 250 constraint functions $x_i^{c\max}(Q_1, Q_2, \dots, Q_M) \leq xw_i, i = 1, \dots, M$. This type of surrogate was chosen
 251 because of its prior success when used with some SBO algorithms for constrained black-box
 252 optimization (e.g. Regis 2011; Regis 2014).

253 For convenience, denote the decision vector of pumping rates by $Q = (Q_1, Q_2, \dots, Q_M)$ and

254 the objective function by $f(Q) = -\sum_{i=1}^M Q_i$, and rewrite each inequality constraint function in

255 the form $g_i(Q) \leq 0$, where $g_i(Q) = x_i^{c\max}(Q) - xw_i$. Now, given the vectors

256 $Q^{(1)}, Q^{(2)}, \dots, Q^{(m)} \in R^M$ (which are simply referred to as points) where the constraint functions
 257 have been evaluated (i.e. so that the values $g_i(Q^{(1)}), g_i(Q^{(2)}), \dots, g_i(Q^{(m)})$ are known for all
 258 $i = 1, \dots, M$), this paper uses an RBF model of the form (Powell, 1992):

259

$$260 \quad S_m(Q) = \sum_{k=1}^m \lambda_k \phi(\|Q - Q^{(k)}\|) + p(Q) \quad (7)$$

261

262 for each of the M inequality constraints. Here, $\phi(r) = r^3$ (the cubic form), $\lambda_1, \dots, \lambda_m \in R$ are
 263 coefficients to be determined, and $p(Q)$ is a linear polynomial whose coefficients also need to
 264 be determined. Training the above RBF surrogate model for a constraint function means
 265 obtaining suitable values for the coefficients of the RBF part and the polynomial part so that
 266 the error between the constraint function and the RBF model at the training points
 267 $Q^{(1)}, Q^{(2)}, \dots, Q^{(m)}$, is minimized. For the particular RBF model and training method used in this
 268 paper, the training error will always be zero, which means that the resulting RBF model passes
 269 through all the data points, that is, the surrogate model is an exact emulator. To obtain the
 270 coefficients in the above cubic RBF model for the i th constraint function g_i , define the matrix

271 $\Phi \in R^{M \times M}$ where $\Phi_{k,l} = \phi(\|Q^{(k)} - Q^{(l)}\|)$ and the matrix $P \in R^{m \times (M+1)}$ whose i th row is

272 $\left[1, (Q^{(i)})^T\right]$. Moreover, define the vector $G_i = \left[g_i(Q^{(1)}), g_i(Q^{(2)}), \dots, g_i(Q^{(m)})\right]^T$. Now, the

273 vector of coefficients $\lambda = [\lambda_1, \dots, \lambda_m]^T$ for the RBF part and the coefficients $c = [c_0, c_1, \dots, c_M]^T$

274 for the polynomial part are obtained by solving the following system of linear equations:

275

$$276 \quad \begin{pmatrix} \Phi & P \\ P^T & 0 \end{pmatrix} \begin{pmatrix} \lambda \\ c \end{pmatrix} = \begin{pmatrix} G_i \\ 0 \end{pmatrix} \quad (8)$$

277

278 Under some simple conditions on the training points, namely that the matrix P has full column
 279 rank, the interpolation matrix in the above system is guaranteed to be invertible (Powell 1992).
 280 Since the above system can be solved quickly and efficiently, even when M is large, the training
 281 time for the cubic RBF model is negligible in comparison to the simulation time needed to
 282 generate the constraint function values. In all, the computational benefits from the negligible

283 training time of cubic RBF models and their exact interpolation characteristics appear attractive
284 for deterministic pumping optimization problems of large dimensionalities.

285

286 **SBO optimization using a prediction-based infill strategy**

287

288 Adaptive SBO methods have successfully applied in problems of pumping optimization of
289 coastal aquifers. Those approaches managed to reduce the number of input-output patterns
290 required from the surrogate model to provide reasonable approximations of the VDST model
291 during optimization (Sreekanth & Datta 2015). Recently, Christelis and Mantoglou (2016a)
292 applied cubic RBF surrogate models for a pumping optimization problem of coastal aquifers,
293 which involved ten pumping wells and ten corresponding constraint functions for each
294 pumping well. In their work, an online training scheme of the RBF models was embedded
295 within the EAS algorithm. Their approach was to add infill points to the initial sampling plan
296 by using the current best solutions found by the RBF model during the optimization operations.
297 This infill strategy favours a fast improvement of the RBF model at the region of the current
298 optimum (local exploitation). However, it neglects the global improvement of the surrogate
299 model and might fail to identify the region of the global optimum (Forrester *et al.* 2008). In
300 that study, the above approach reduced by 96% the corresponding computational time with the
301 VDST-EAS approach while it successfully located the region of the global optimum. We apply
302 the same method here, in order to test its performance as a basic SBO strategy and evaluate its
303 performance for problems of larger dimensions and under limited computational budgets. The
304 steps of the method, denoted hereinafter as RBF-EAS, are briefly presented below since the
305 details have been presented in Christelis & Mantoglou (2016a):

- 306 1. Use a Latin Hypercube Sampling method to produce the initial population for the EAS
307 algorithm and evaluate the VDST model at these points.
- 308 2. Store the initial sampling plan of the evaluation points $Q^{(1)}, Q^{(2)}, \dots, Q^{(m)}$, along with the
309 responses of the VDST model for the constraint functions $g_i(Q), i = 1, \dots, M$ and train
310 the RBF surrogate models.
- 311 3. Run EAS algorithm based on the RBF models and if a new optimum is found, use the
312 VDST model to evaluate the current best solution Q . Add the new input-output data to
313 the initial sampling plan, and re-train the RBF models.
- 314 4. Is the computational budget exhausted? If yes, return final solution, else go to step 3.

315 **The ConstrLMSRBF algorithm**

316

317 The ConstrLMSRBF algorithm (Regis 2011) is an SBO algorithm for constrained black-box
318 optimization that uses the RBF interpolation model described previously, to approximate the
319 black-box objective and inequality constraint functions. In the case of the pumping
320 optimization problem in (5), only the constraint functions are computationally expensive to
321 evaluate. However, in the standard implementation of ConstrLMSRBF, the algorithm also
322 maintains an RBF surrogate model for the objective function. In this case though, since the
323 objective function is linear in the decision variables (the pumping rates), one can
324 mathematically prove that the resulting surrogate will also be linear and will be identical to the
325 objective function, provided there are at least $M + 1$ training points.

326 ConstrLMSRBF begins by evaluating the objective and constraint functions at a feasible
327 starting point and at the points of a space-filling design, specifically a Latin hypercube design
328 (LHD) with $2M + 1$ points, over the region defined by the bound constraints of the problem
329 $[Q_{\min}, Q_{\max}]$. Together, the feasible starting point and the LHD points constitute the initial
330 training points. The space-filling design points possibly include infeasible points, and for the
331 version of ConstrLMSRBF used in this paper, the first initial point must be feasible. The
332 requirement of having a feasible point is not unreasonable since in many applications a feasible
333 solution is often available or easy to obtain, as is the case for the above pumping optimization
334 problem, and the practitioner is simply looking to improve this feasible solution. However, an
335 extension of ConstrLMSRBF in Regis (2014) allows all initial points to be infeasible.

336 After evaluating the objective and inequality constraint functions at the initial points, RBF
337 models are fit for the objective and constraint functions using all available data points. Then
338 the algorithm goes through a loop that involves generating a large number of random candidate
339 points obtained by perturbing some (or all) of the coordinates of the current best feasible point
340 using Gaussian distributions with zero mean and with standard deviations that are allowed to
341 vary adaptively depending on performance, to facilitate either local search or global search.
342 When generating a candidate point, the choice of which coordinates of the current best point
343 are perturbed is random, and is controlled by a parameter p_{select} which is the probability that a
344 given coordinate is perturbed. In the numerical experiments, p_{select} equals 0.5 or 1. Next, the
345 algorithm gathers the candidate points that are predicted to be feasible or that have the
346 minimum number of predicted constraint violations. These points will be referred to as the
347 valid candidate points. The next point where the simulation will be run (or where objective and

348 constraint functions will be evaluated) is chosen to be the best point among all the valid
 349 candidate points according to two criteria: predicted objective function value of the candidate
 350 point according to the RBF model of the objective, and its minimum distance from previously
 351 evaluated points. More precisely, for each valid candidate point Q , the algorithm calculates a
 352 score for the RBF criterion, $V_{RBF}(Q)$, and a score for the distance criterion, $V_{DIST}(Q)$. These
 353 scores vary from 0 to 1, with the preferred candidate points having scores closer to zero. Then,
 354 the next point where the simulation will take place is the valid candidate point Q that
 355 minimizes the value of:

$$356 \quad V(Q) = w_{RBF} V_{RBF}(Q) + w_{DIST} V_{DIST}(Q) \quad (9)$$

357
 358 where w_{RBF} and w_{DIST} are the weights for the two criteria and they satisfy $w_{RBF} + w_{DIST} = 1$. In
 359 the numerical experiments, these weights were fixed to $w_{RBF} = 0.95$ and $w_{DIST} = 0.05$ to put
 360 more emphasis on the RBF criterion.
 361

362 Once the VDST simulation has taken place at the selected valid candidate point, the
 363 algorithm re-trains the RBF surrogate model with the new data point. Then it goes back to
 364 generating a new set of random candidate points and continues in the same manner as before
 365 until the computational budget is exhausted (e.g. the maximum number of VDST simulations
 366 has been reached). More details on ConstrLMSRBF can be found in Regis (2011).

367 **Problem settings**

368
 369 Four pumping optimization problems of different dimensionality were solved to test the
 370 performance of the algorithms described above. That is, $M = 10$, $M = 20$, $M = 30$ and
 371 $M = 40$. For each increase in the number of pumping wells the total recharge of the coastal
 372 aquifer model was also modified accordingly. This facilitated the comparison on the
 373 performance of the algorithms by moving the region of the global optimum in a different
 374 location. Therefore, for $M = 10$ the total recharge was set to $5409.86 m^3/day$, for $M = 20$ the
 375 total recharge was set to $6159.8 m^3/day$, for $M = 30$ the total recharge was set to
 376 $6909.8 m^3/day$ and for $M = 40$ the total recharge was set to $7659.8 m^3/day$. For each
 377 optimization problem (due to the different total recharge rates) an initial VDST model run was
 378 performed with no pumping present, until the head and salinity concentration fields reached
 379

380 steady-state. These were used as the initial conditions for the subsequent VDST simulations
381 during the optimization task.

382 Each optimization problem was solved based on a specified budget of VDST simulations.
383 The maximum allowed number of VDST model runs was set to $100 \times M$. Since the
384 optimization methods of this study are based on stochastic operators, a set of 30 independent
385 optimization runs is used for each approach in order to perform an adequate statistical
386 comparison. In addition, for each independent optimization run a new initial population is
387 generated which is applied to all the optimization methods to ensure same starting conditions.

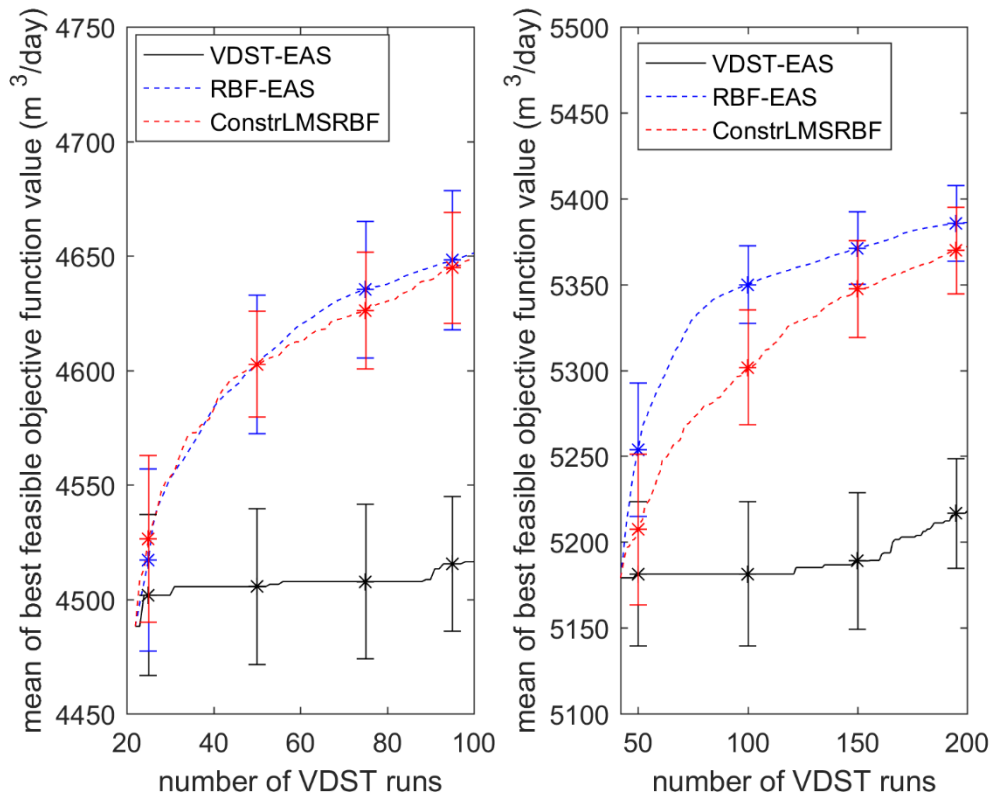
388

389 RESULTS AND DISCUSSION

390

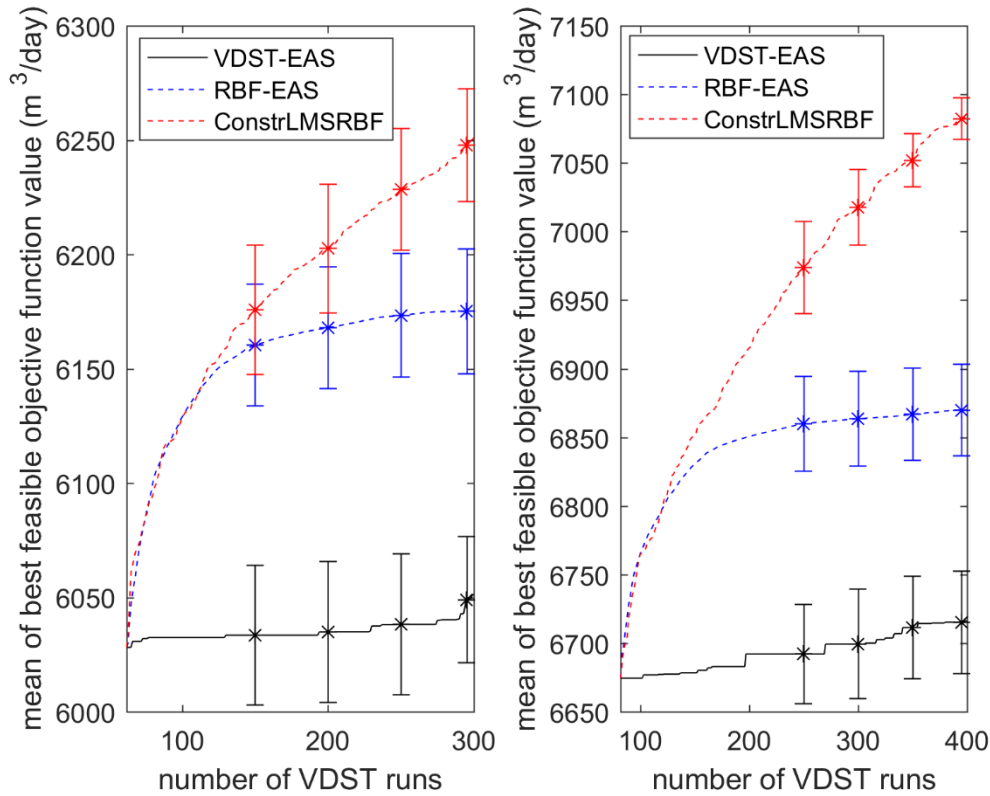
391 Figures 3 and 4 present the performance of the optimization methods based on their best
392 average feasible objective function value among the 30 independent runs. The problems
393 considering 10 and 20 pumping wells are considered of moderate dimensionality and are
394 grouped together. The problems with 30 and 40 pumping wells are considered as of larger
395 dimensionality and are also grouped together.

396



397

398 [FIGURE 3]



400

401

402 [FIGURE 4]

403

404 Results demonstrate that the SBO methods outperform the direct VDST-EAS optimization for
 405 all test problems. The SBO methods were able to improve the objective function value given
 406 the available number of runs with the VDST model. The more global search capabilities of
 407 ConstrLMSRBF against the predictive-based infill strategy of EAS-RBF algorithm are also
 408 demonstrated, particularly for the higher dimensional problems (figure 4). In both SBO
 409 frameworks, the objective function value exhibits a rapid improvement after the initial
 410 population evaluation comparative to VDST-EAS. However, in problems where $M = 30$ and
 411 $M = 40$, RBF-EAS appears to stall as the computational budget is exhausted. On the other
 412 hand, ConstrLMSRBF displays a continuous improvement of the average objective function
 413 value as the number of VDST runs are increased for all problems. A one-way analysis of
 414 variance (ANOVA) test was also performed on the above samples using the built-in MATLAB
 415 functions *anova1* and *multcompare* (Statistics and Machine Learning Toolbox, 2016b). The
 416 results are shown in the following table.

417

418 [TABLE 1]

Optimization frameworks		p-value			
		M=10	M=20	M=30	M=40
VDST-EAS	RBF-EAS	3.365-07	1.053-09	4.088-08	6.424-08
VDST-EAS	ConstrLMSRBF	5.158-07	2.812-09	9.561-10	9.560-10
RBF-EAS	ConstrLMSRBF	0.994	0.798	0.0021	9.569-10

419

420 It is demonstrated that the p-values between VDST-EAS and the two SBO strategies are close
 421 to zero for all optimization problems which confirms that the difference in their sample mean
 422 values is statistically significant. Furthermore, the comparison between RBF-EAS and
 423 ConstrLMSRBF shows that the sample means of the two methods for the 30 and the 40 decision
 424 variable problems are also significantly different.

425

426 **CONCLUSIONS**

427

428 A single-objective pumping optimization problem of coastal aquifer was solved using both
 429 direct and surrogate-based optimization methods. The direct optimization (VDST-EAS)
 430 involved the combination of a variable density and salt transport numerical model with an
 431 evolutionary algorithm. The two SBO methods were applied by utilizing the same surrogate
 432 models, namely, cubic RBF models. However, they were based on different update strategies
 433 for the surrogate model. The first (RBF-EAS) employed a classic prediction-based infill
 434 strategy (local exploitation) embedded in the same evolutionary algorithm with the direct
 435 optimization framework. The second (ConstrLMSRBF) was based on a comprehensive infill
 436 strategy which aims at both local exploitation and global exploration of the decision variable
 437 space.

438 To the best of our knowledge, this is the first time in coastal aquifer management that
 439 optimization problems of moderate and large dimensionalities are employed and compared for
 440 both direct and SBO methods. It is also the first time that a comprehensive generic SBO method
 441 (ConstrLMSRBF algorithm) is tested for single-objective pumping optimization problems of
 442 coastal aquifers. Results demonstrated an outperformance of the SBO methods against the
 443 direct optimization for the case of four different optimization problems with increased
 444 dimensionality (from 10 to 40 pumping wells). In particular, ConstrLMSRBF algorithm is
 445 considered a promising SBO method for coastal aquifer management since located the best
 446 solutions under limited computational budgets and demonstrated a robust performance for all
 447 optimization problems. The ANOVA tests confirmed the statistical significance of the

448 differences in the sample means between the direct optimization and the SBO methods.
449 Furthermore, the simple and fast implementation of cubic RBF surrogate models, in both SBO
450 approaches, facilitated the individual treatment of a large number of constraint functions (up
451 to 40) in negligible computational cost.

452

453 REFERENCES

454

455 Asher, M. J., Croke, B. F. W., Jakeman, A.J. & Peeters, L. J. M. 2015 A review of surrogate
456 models and their application to groundwater modelling. *Water Resour. Res.* **51**(8), 5957-5973.

457 Ataie-Ashtiani, B., Ketabchi, H. & Rajabi, M. M. 2014 Optimal management of a freshwater
458 lens in a small island using surrogate models and evolutionary algorithms. *J. Hydrolog. Eng.*
459 **19**, 339-354.

460 Bhattacharjya, R. K. & Datta, B. 2005 Optimal management of coastal aquifers using linked
461 simulation optimization approach. *Water Resour. Manage.* **19**(3), 295-320.

462 Christelis, V. & Mantoglou, A. 2016a Pumping optimization of coastal aquifers assisted by
463 adaptive metamodelling methods and radial basis functions. *Water Resour. Manage.*
464 Doi:10.1007/s11269-016-1337-3.

465 Christelis, V. & Mantoglou, A. 2016b Coastal aquifer management based on the joint use of
466 density-dependent and sharp interface models. *Water Resour. Manage.* **30**(2), 861-876.

467 Dhar, A. & Datta, B. 2009 Saltwater intrusion management of coastal aquifers, I: linked
468 simulation-optimization. *J. Hydrolog. Eng.* **14**, 1263–1272.

469 Efstratiadis, A. & Koutsoyiannis, D. 2002 An evolutionary annealing-simplex algorithm for
470 global optimization of water resource systems. *Proceedings of the Fifth International*
471 *Conference on Hydroinformatics*, Cardiff, UK, International Water Association Publishing **2**,
472 1423-1428.

473 Forrester, A. I. J., Sobester, A. & Keane, A. J. 2008 *Engineering design via surrogate*
474 *modelling-A practical guide*. Wiley, New York.

475 Forrester, A. I. J. & Keane, A. J. 2009 Recent advances in surrogate-based optimization. *Prog.*
476 *Aerosp. Sci.* **49**, 50-79.

477 Giambastiani, B. M., Antonellini, M., Essink, G. H. O. & Stuurman, R. J. 2007 Saltwater
478 intrusion in the unconfined coastal aquifer of Ravenna (Italy): a numerical model. *J. Hydrol.*
479 **340**(1), 91-104.

480 Gingerich, S. B. & Voss, C. I. 2005 Three-dimensional variable-density flow simulation of a
481 coastal aquifer in southern Oahu, Hawaii, USA. *Hydrogeol. J.* **13**(2), 436-450.

482 Graf, T. & Therrien, R. 2005 Variable-density groundwater flow and solute transport in porous
483 media containing nonuniform discrete fractures. *Adv. Water Resour.* **28**, 1351-1367.

484 Hussain, M. S., Javadi, A. A., Ahangar-Asr, A. & Farmani, R. 2015 A surrogate model for
485 simulation–optimization of aquifer systems subjected to seawater intrusion. *J. Hydrol.* **523**,
486 542-554.

487 Jones, D., Schonlau, M. & Welch, W. 1998 Efficient global optimization of expensive black-
488 box functions. *J. Global Optim.* **13**, 455-492.

489 Karpouzou, D. K. & Katsifarakis, K. L. 2013 A set of new benchmark optimization problems
490 for water resources management. *Water Resour. Manage.* **27**(9), 3333-3348.

491 Kerrou, J., Renard, P., Cornaton, F. & Perrochet, P. 2013 Stochastic forecasts of seawater
492 intrusion towards sustainable groundwater management: application to the Korba aquifer
493 (Tunisia). *Hydrogeol. J.* **21**(2), 425-440.

494 Ketabchi, H. & Ataie-Ashtiani, B. 2015 Evolutionary algorithms for the optimal management
495 of coastal groundwater: A comparative study toward future challenges. *J. Hydrol.* **520**, 193-
496 213.

497 Kolditz, O., Ratke, R., Diersch, H. J. G., & Zielke, W. 1998 Coupled groundwater flow and
498 transport: 1. Verification of variable density flow and transport models. *Adv. Water Resour.*
499 **21**(1), 27-46.

500 Kopsiaftis, G., Mantoglou, A. & Giannouloupolous, P. 2009 Variable density coastal aquifer
501 models with application to an aquifer on Thira Island. *Desalination* **237**(1), 65-80.

502 Kourakos, G., & Mantoglou, A. 2009. Pumping optimization of coastal aquifers based on
503 evolutionary algorithms and surrogate modular neural network models. *Adv. Water Resour.*
504 **32**(4), 507-521.

505 MATLAB, Statistics and Machine Learning Toolbox, Release 2016b. The MathWorks, Inc.,
506 Natick, Massachusetts, United States.

507 Mantoglou, A., Papantoniou, M. & Giannouloupolous, P. 2004 Management of coastal aquifers
508 based on nonlinear optimization and evolutionary algorithms. *J. Hydrol.* **297**(1–4), 209–228.

509 Mantoglou, A. & Papantoniou, M. 2008 Optimal design of pumping networks in coastal
510 aquifers using sharp interface models. *J. Hydrol.* **361**, 52–63.

511 Mugunthan, P., Shoemaker, C. A., & Regis, R. G. 2005. Comparison of function
512 approximation, heuristic and derivative-based methods for automatic calibration of
513 computationally expensive groundwater bioremediation models. *Water Resour. Res.*
514 Doi:10.1029/2005WR004134.

515 Papadopoulou, M. P., Nikolos, I. K., & Karatzas, G. P. 2010. Computational benefits using
516 artificial intelligent methodologies for the solution of an environmental design problem:
517 saltwater intrusion. *Water Sci. Technol.* **62**(7), 1479-1490.

518 Parr, J. M., Keane, A. J., Forrester, A. I., & Holden, C. M. E. 2012. Infill sampling criteria for
519 surrogate-based optimization with constraint handling. *Eng. Optimiz.* **44**(10), 1147-1166.

520 Pool, M. & Carrera, J. 2011 A correction factor to account for mixing in Ghyben-Herzberg and
521 critical pumping rate approximations of seawater intrusion in coastal aquifers. *Water Resour.*
522 *Res.*, **47**(5).

523 Powell, M. J. D. 1992. *The theory of Radial Basis Function Approximation in 1990*, in: Light,
524 W. (ed.), *Advances in Numerical Analysis, Volume 2: Wavelets, Subdivision Algorithms and*
525 *Radial Basis Functions*, pp. 105–210, Oxford University Press.

526 Rao, S. V. N., Sreenivasulu, V., Bhallamudi, S. M., Thandaveswara, B. S. & Sudheer, K.P.
527 2004 Planning groundwater development in coastal aquifers. *Hydrol. Sci. J.* **49**(1).

528 Razavi, S., Tolson, B. A. & Burn, D. H. 2012a Review of surrogate modelling in water
529 resources. *Water Resour. Res.* **48**(7).

530 Razavi, S., Tolson, B. A. & Burn, D. H. 2012b Numerical assessment of metamodelling
531 strategies in computationally intensive optimization. *Environ. Modell. Softw.*, **34**, 67-86.

532 Regis, R. G. & Shoemaker, C. A. 2005 Constrained global optimization of expensive black box
533 functions using radial basis functions. *J. Global Optim.* **31**, 153-171.

534 Regis, R. G. & Shoemaker, C. A. 2007 Improved strategies for radial basis function methods
535 for global optimization. *J. Global Optim.* **37**, 113-135.

536 Regis, R. G. 2011 Stochastic radial basis function algorithms for large-scale optimization
537 involving expensive black-box objective and constraint functions. *Comput. Oper. Res.* **38**, 837-
538 853.

539 Regis, R. G. & Shoemaker, C. A. 2013 A quasi-multistart framework for global optimization
540 of expensive functions using response surface methods. *J. Global Optim.* **56**, 1719-1753.

541 Regis, R.G. 2014 Evolutionary programming for high-dimensional constrained expensive
542 black-box optimization using radial basis functions. *IEEE T. Evolut. Comput.* **18**(3).

543 Regis, R. G. & Shoemaker, C.A. 2013 Combining radial basis function surrogates and dynamic
544 coordinate search in high-dimensional expensive black-box optimization. *Eng. Optimiz.* **45**(5),
545 529-555.

546 Rozos, E., Efstratiadis, A., Nalbantis, I. & Koutsoyiannis, D. 2004 Calibration of a semi-
547 distributed model for conjunctive simulation of surface and groundwater flows. *Hydrol. Sci. J.*
548 **49**(5), 819-842.

549 Roy, T., Schütze, N., Grundmann, J., Brettschneider, M. & Jain, A. 2016 Optimal groundwater
550 management using state-space models: a case study for an arid coastal region. *J. Hydroinf.*
551 **18**(4), 666-686.

552 Solomatine, D. P. & Ostfeld, A. 2008 Data-driven modelling: some past experiences and new
553 approaches. *J. Hydroinf.* **10** (1), 3-22.

554 Sreekanth, J. & Datta, B. 2011 Comparative evaluation of Genetic Programming and Neural
555 Network as potential surrogate models for coastal aquifer management. *Water Resour.*
556 *Manage.* **25**, 3201-3218.

557 Sreekanth, J. & Datta, B. 2015 Review: simulation-optimization models for the management
558 and monitoring of coastal aquifers. *Hydrogeol. J.* **23**(6), 1155-1166.

559 Therrien, R. & Sudicky, E. A. 1996 Three-dimensional analysis of variably-saturated flow and
560 solute transport in discretely-fractured porous media. *J. Contam. Hydrol.* **23**, 1-44.

561 Therrien, R., McLaren, R. G., Sudicky, E. A. & Panday, S. M. 2006 *HydroGeoSphere-A three-*
562 *dimensional numerical model describing fully-integrated subsurface and surface flow and*
563 *solute transport. Groundwater Simulations Group, University of Waterloo, Canada, 2006.*

564 Thompson, C., Smith, L. & Maji, R, 2007 Hydrogeological modelling of submarine
565 groundwater discharge on the continental shelf of Louisiana. *J. Geophys. Res.* Doi:
566 10.1029/2006JC003557.

567 Tsoukalas, I., Kossieris, P., Efstratiadis, A. & Makropoulos, C. 2016 Surrogate-enhanced
568 evolutionary annealing simplex algorithm for effective and efficient optimization of water
569 resources problems on a budget. *Environ. Modell. Softw.* **77**, 122-142.

570 Voss, C. I. & Souza, W. R. 1987 Variable density flow and solute transport simulation of
571 regional aquifers containing a narrow freshwater- saltwater transition zone. *Water Resour.*
572 *Res.* **23**(10), 1851-1866.

573 Werner, A. D., Bakker, M., Post, V. E. A., Vandenbohede, A, Lu, C., Ataie-Ashtiani, B.,
574 Simmons, C. T. & Barry D. A. 2013 Seawater intrusion processes, investigation and
575 management: Recent advances and future challenges. *Adv. Water Resour.* **51**, 3-26.